

Primordial Black Holes and Primordial Nucleosynthesis I: Effects of Hadron Injection from Low Mass Holes

K. Kohri

*Research Center for the Early Universe, Faculty of Science, The University of Tokyo, Tokyo
113-0033, Japan*

Jun'ichi Yokoyama

*Department of Earth and Space Science, Graduate School of Science, Osaka University,
Toyonaka, 560-0043, Japan*

Abstract

We investigate the influence of hadron injection from evaporating primordial black holes (PBHs) in the early stage of the primordial nucleosynthesis era ($t \simeq 10^{-3} - 10^4$ sec). The emitted quark-antiquark pairs or gluons immediately fragment into a lot of hadrons and scatter off the thermal plasma which is constituted by photons, electrons and nucleons. For the relatively low mass holes we point out that the dominant effect is the inter-conversion between ambient proton and neutron through the strong interaction induced by the emitted hadrons. Even after the freeze-out time of the weak interactions between neutron and proton, more neutrons are produced and the synthesized light element abundances could be drastically changed. Comparing the theoretical predictions with the observational data, we constrain the PBH's density and their lifetime. We obtain the upper bound for PBH's initial mass fraction, $\beta \lesssim 10^{-20}$ for $10^8 \text{g} \lesssim M \lesssim 10^{10} \text{g}$, and $\beta \lesssim 10^{-22}$ for $10^{10} \text{g} \lesssim M \lesssim 3 \times 10^{10} \text{g}$.

98.80.Cq, 98.80.Ft, 04.70.Bw, 26.35.+c, OU-TAP 101

arXiv:astro-ph/9908160v1 16 Aug 1999

I. INTRODUCTION

Primordial black holes (PBHs) are formed in the hot early Universe if overdensity of order of unity exists and a perturbed region enters the Hubble radius [1]. They serve as a unique probe of primordial density fluctuations on small scales. For example, if massive compact halo objects (MACHOs) [2] found by gravitational microlensing observation toward the Large Magellanic Clouds turn out to be the PBHs, which originate from density fluctuations generated during inflation, we can determine model parameters of the inflation model with high accuracy [3]. In fact, this possibility is attracting more attention these days because none of the conventional candidates of MACHOs are plausible from various astrophysical considerations and observations.

Even the nonexistence of PBHs over some mass ranges, however, would provide useful informations on the primordial spectrum of density fluctuations. In this sense it is very important to obtain accurate constraints on the abundance of PBHs on each mass scale.

Cosmological constraints on the mass spectrum of the PBHs can be classified to three classes. The first one applies to heavy black holes with mass $M > 4 \times 10^{14}$ g which have not evaporated by now. Current mass density of such holes should not exceed the total mass density of the universe. More stringent constraints are obtained from the microlensing experiments on holes with sub-solar masses [2]. The second class is due to the radiation of high energy particles from evaporating black holes [4,5]. Various constraints have been imposed from primordial big-bang nucleosynthesis (BBN) [6–10], microwave background radiation [11], and gamma-ray background radiation [12]. Finally, there may be yet another class of constraints if PBHs do not evaporate completely but leave relics with mass of order of the Planck mass or larger [13]. Their mass density should remain small enough.

The purpose of this paper is to reanalyze the effects of evaporating primordial black holes on BBN in order to improve constraints on their mass spectrum. Although extensive work was done on this issue in 1970s just after the idea of PBH was proposed, to our knowledge, it has not been studied almost two decades now, and old constraints are still used in the literature [14,15]. In order to compare the previous work with the modern view of BBN and high energy physics, we start with a brief review of what has been done on the subject.

Vainer and Nasel'skii [6] studied the effects of the injection of high-energy neutrinos and antineutrinos which change the epoch of the freeze out of the weak interactions and also the neutron-to-proton ratio at the onset of the nucleosynthesis. This results in the increase of ${}^4\text{He}$. Demanding that its primordial abundance, Y_p , should satisfy $Y_p < 0.33$, they concluded the ratio of the energy density of PBHs to that of baryons should be smaller than $10 - 10^4$ for holes with mass $M = 10^9 - 3 \times 10^{11}$ g. This approximately corresponds to $\beta(M) < 10^{-22} - 10^{-19}$, where $\beta(M)$ is the initial fraction of PBHs with mass M to the total energy density of the universe when the horizon mass is equal to M , *i.e.* $\beta(M) \equiv (\rho_{\text{BH}}/\rho_{\text{tot}})_i$. These authors also studied the effects of entropy generation from PBHs but they obtained a modest constraint that the energy density of the relevant holes should be smaller than that of the photons at evaporation.

More detailed numerical analysis of the latter effect was done by Miyama and Sato [7], who calculated the effect of entropy production from PBHs with mass $M = 10^9 - 10^{13}$ g evaporating during or after the nucleosynthesis. If these PBHs were too abundant, the baryon-to-entropy ratio at the nucleosynthesis should be increased which would result in

overproduction of ${}^4\text{He}$ and underproduction of D. They demanded that $Y_p < 0.29$ and that mass fraction of D should be larger than 1×10^{-5} . If we approximate their result with a single power law, we find

$$\beta(M) < 10^{-15} M_{10}^{-5/2}, \quad (1)$$

for $M = 10^9 - 10^{13}$ g, where $M_{10} \equiv M/10^{10}$ g.

Zel'dovich et al [8], on the other hand, studied the effect of emission of high-energy nucleons and antinucleons from PBHs. They claimed such emission would increase deuterium abundance due to capture of free neutrons by protons and spallation of ${}^4\text{He}$ by emitted particles. Their conclusions were

$$\begin{aligned} \beta(M) &< 6 \times 10^{-18} M_{10}^{-1/2}, & \text{for } M = 10^9 - 10^{10}\text{g}, \\ &< 6 \times 10^{-22} M_{10}^{-1/2}, & \text{for } M = 10^{10} - 5 \times 10^{10}\text{g}, \\ &< 3 \times 10^{-23} M_{10}^{5/2}, & \text{for } M = 5 \times 10^{10} - 5 \times 10^{11}\text{g}, \\ &< 3 \times 10^{-21} M_{10}^{-1/2}, & \text{for } M = 10^{11} - 10^{13}\text{g}. \end{aligned} \quad (2)$$

Vainer, Dryzhakova, and Nasel'skii [9] then performed numerical integration of nucleosynthesis network in the presence of neutron-antineutron injection, taking the neutron lifetime to be $918(\pm 14)$ sec and using the observational data $Y_p = 0.29 \pm 0.04$ and the mass fraction of D to be 5×10^{-5} . They calculated spallation of ${}^4\text{He}$ and resultant extra production of D assuming that PBHs were produced out of scale-invariant density fluctuations. As a result they obtained the constraint $\beta < 10^{-26}$ for the relevant mass range.

Lindley [10] considered another effect of evaporating PBHs with mass $M > 10^{10}$ g, namely, photodissociation of deuterons produced in the nucleosynthesis. He found the constraint $\beta \lesssim 3 \times 10^{-20} M_{10}^{1/2}$, and concluded that photodestruction was comparable to the extra production of deuterons discussed in [8].

Since these papers were written, both observational data of light elements and the neutron lifetime have changed considerably [16]. More important, however, is the change in our view of high energy physics of the energy scale relevant to PBHs evaporating in the nucleosynthesis era. That is, hadrons are not emitted in the form of nucleons or mesons but as a quark-gluon jet in the modern view of quantum chromodynamics (QCD). Thus we should adopt the Elementary Particle Picture of Carr [5] and assume that elementary particles in the standard model are emitted from PBHs and they generate jets. In fact, the number of jet-generated particles far exceeds that of directly emitted counterparts. In this sense the previous calculation of BBN in the presence of evaporating PBHs should be entirely revised. The above procedure has already been taken in the analysis of cosmic rays from evaporating PBHs [17]. We incorporate emission of various hadrons from PBH-originated jets to BBN for the first time.

We adopt a simple and conventional view that PBHs are produced with a single mass, M , when the horizon mass is equal to M , namely at $t = 2.4 \times 10^{-29} M_{10} \text{ sec} \equiv t_{form}$, and obtain an improved constraints on their initial abundance at each mass scale. Recent numerical calculations of PBH formation, however, have revealed the mass spectrum of PBHs spreads rather widely even if the spectrum of primordial density fluctuation is sharply peaked on a specific scale [18,19]. In particular, the authors of [18] discovered the critical behavior and its cosmological consequences have been discussed in [20]. By convolving our results with

the mass functions obtained in these papers, one can obtain constraints on PBH formation in more realistic situations.

When PBHs evaporate and emit various particles in BBN epoch, *i.e.* at $T = 10\text{MeV} - 1\text{keV}$, such high energy particles interact with the ambient photons, electrons and nucleons and they finally transfer all the kinetic energy into the thermal bath through the electromagnetic interaction or the strong interaction. Through the above process, such dangerous high energy particles possibly induce the various effects on the background and change the standard scenario considerably.

Once quark-antiquark pairs or gluons are emitted from a PBH, a lot of hadrons, *e.g.* pions, kaons and nucleons (protons and neutrons) are produced through their hadronic fragmentation. They inter-convert the ambient protons and neutrons each other through the strong interaction. If the inter-conversion rate between neutrons and protons becomes large again after the freeze-out time of the weak interactions in the standard BBN (SBBN) or $t \simeq 1\text{sec}$, the protons which are more abundant than the neutrons at that time are changed into neutrons. That is, this results in an excess of neutrons compared with SBBN. Therefore, the hadron injection significantly influences the freeze-out value of the neutron-to-proton ratio and the final abundances of ^4He , D and ^7Li are drastically changed. In this case it is expected that both ^4He and D tend to become more abundant than in SBBN. If PBHs are so massive that they continue to emit particles even after ^4He are produced, then spallation of ^4He due to high energy particles will tend to increase the final D ¹. In this paper, as a first step of the full analysis, we concentrate on the low-mass PBHs and consider only the former effects. The latter issue will be addressed in a separate publication [25].

Reno and Seckel [26] investigated the detail of the physical mechanism and the influences of the hadron injection from long-lived massive decaying particles on BBN. They constrained the parent particle's lifetime and the number density comparing the theoretical prediction of the light element abundances with the observational data. Here we basically follow their treatment and apply it to the hadron injection originated in the PBH evaporation.

The rest of the paper is organized as follows. In §II, we review properties of black hole evaporation and jets. In §III formulation to calculate the effect of hadron injection to BBN is given and observational data of light element abundances are summarized. The result is presented in §IV. Finally §V is devoted to the conclusion. We use the units $c = \hbar = k_B = 1$.

II. EVAPORATION AND JETS

First we briefly summarize basic results of PBH evaporation. As was first shown by Hawking [4], a black hole with mass M emits thermal radiation with the temperature given by

$$T_{\text{BH}} = \frac{1}{8\pi GM} = 1.06M_{10}^{-1}\text{TeV}. \quad (3)$$

More precisely, a neutral non-rotating black hole emits particles with energy between Q and $Q + dQ$ at a rate

¹This situation has been studied in [24] in the context of late-decaying particles.

$$d\dot{N}_s = \frac{\Gamma_s dQ}{2\pi} \frac{1}{e^{(Q/T_{\text{BH}})} - (-1)^{2s}}, \quad (4)$$

where s is the spin of the emitted particle. Γ_s is its dimensionless absorption coefficient whose functional shape is found in [21]. It is related with the absorption cross section $\sigma_s(M, Q)$ as $\Gamma_s(M, Q) = Q^2 \sigma_s(M, Q)/\pi$. In the high-energy limit $Q \gg T$, σ_s approaches to the geometric optics limit $\sigma_g \equiv 27\pi G^2 M^2$.

The average energies of a neutrino, an electron, and a photon are given by $E_\nu = 4.22T_{\text{BH}}$, $E_e = 4.18T_{\text{BH}}$, and $E_\gamma = 5.71T_{\text{BH}}$, respectively. The peak energy of the flux and that of the power are within 7% of the above values [22]. Averaging over degrees of freedoms of quarks and gluons in the standard model, we find the average energy $\bar{E} = 4.4T_{\text{BH}}$.

MacGibbon elaborated on the lifetime of a PBH, τ_{BH} , summing up the contribution of all the emitted particles and integrating the mass loss rate

$$\frac{dM_{10}}{dt} = -5.34 \times 10^{-5} f(M) M_{10}^{-2} \text{ sec}^{-1}, \quad (5)$$

over the lifetime [23]. The result is approximately given by

$$\tau_{\text{BH}} = 6.24 \times 10^3 f(M)^{-1} M_{10}^3 \text{ sec}. \quad (6)$$

Here $f(M)$ is a function of the number of emitted particle species normalized to unity for $M \gg 10^{17}\text{g}$ holes which emit only photons, three generations of neutrinos and anti-neutrinos, and gravitons. Depending on the spin s , each relativistic degree of freedom contributes to $f(M)$ as [23]

$$\begin{aligned} f_{s=0} &= 0.267, & f_{s=1} &= 0.060, & f_{s=3/2} &= 0.020, & f_{s=2} &= 0.007, \\ f_{s=1/2} &= 0.147 \text{ (neutral)}, & f_{s=1/2} &= 0.142 \text{ (charge} = \pm e\text{)}. \end{aligned} \quad (7)$$

Summing up contributions of all the particles in the standard model, we find $f(M) = 14.34$. In this case the lifetime reads

$$\tau_{\text{BH}} = 435 M_{10}^3 \text{ sec}, \quad (8)$$

or

$$M = 1.32 \times 10^9 \left(\frac{\tau_{\text{BH}}}{1 \text{ sec}} \right)^{\frac{1}{3}} \text{ g}. \quad (9)$$

Thus a PBH evaporating by the end of BBN $t \simeq 10^3 \text{ sec}$ has a mass $M \lesssim 10^{10}\text{g}$ and the temperature $T_{\text{BH}} \gtrsim 1\text{TeV}$.

For such a PBH with temperature higher than the QCD scale, $\Lambda_{\text{QCD}} \sim 10^{2.5}\text{MeV}$, it has been argued [22] that particles radiated from it can be regarded as asymptotically free at emission. The emitted quarks and gluons fragment into further quarks and gluons until they cluster into the observable hadrons when they have traveled a distance $\Lambda_{\text{QCD}}^{-1} \sim 10^{-13}\text{cm}$. The hadron jet thus produced would be similar to that produced in e^+e^- annihilation.

We now estimate the average number of the emitted hadron species H_i per jet as

$$N^{H_i} = f_{H_i} \frac{\langle N_{ch} \rangle}{2}, \quad (10)$$

where $\langle N_{ch} \rangle$ is the averaged charged-particle multiplicity which represents the total number of the charged particles emitted per two hadron jets, f_{H_i} is the number fraction of the hadron species H_i to all the emitted charged particles.

It is reasonable to assume that the averaged charged-particle multiplicity is independent of the source of the hadron jet. In this paper we use the data obtained by the e^+e^- collider experiments and extrapolate it to higher energy scales. A number of experimental data are available at least up to $\sqrt{s} \simeq 100$ GeV where \sqrt{s} denotes the center of mass energy. Recently LEP II experiments (ALEPH, DELPHI, L3 and OPAL) yielded useful data for $\sqrt{s} = 130 - 172$ GeV. One can fit the data by a function, $\langle N_{ch} \rangle = a + b \exp(c\sqrt{\ln(s/\Lambda^2)})$, where Λ is the cut-off parameter in the perturbative calculations associated with the onset of the hadronization and a , b and c are constants [27]. The above functional shape is motivated by the next-to-leading order perturbative QCD calculations. We fit the data of the e^+e^- collider experiments for $\sqrt{s} = 1.4 - 172$ GeV [28] and we find

$$\langle N_{ch} \rangle = 1.73 + 0.268 \exp\left(1.42\sqrt{\ln(s/\Lambda^2)}\right), \quad (11)$$

with $\chi^2 = 90.3$ for 93 data points and the error of the fitting is about 10%. Here we have taken $\Lambda = 1$ GeV. We assigned systematic errors of 10% for $\sqrt{s} = 1.4 - 7.8$ GeV because MARK I and $\gamma\gamma 2$ experiments do not include the systematic errors in their data, see [28]. In Fig. 1 we plot $\langle N_{ch} \rangle$ for the center of mass energy \sqrt{s} . When we apply the results of the e^+e^- collider experiments to the case of PBH evaporation, we take $\sqrt{s} = 2\bar{E}$ as the energy of two hadron jets from the PBH evaporation because we assume that two hadron jets are induced per one quark-antiquark pair emission here. Then we can approximately estimate the average energy of an emitted hadron species H_i as $E_{H_i} \simeq \bar{E}/\langle N_{ch} \rangle$.

The next issue is to find f_{H_i} . In this paper we adopt the experimental data of f_{H_i} at $\sqrt{s} = 91.2$ GeV, which is the highest energy for which these data are available [28], and we assume that f_{H_i} do not change significantly in the energy range $\sqrt{s} \simeq 100$ GeV - 20 TeV.² From the table of f_{H_i} in [28] we must estimate effective f_{H_i} for each hadron species on the relevant time scale. That is, we must also take into account the decay products of those particles whose lifetime is too short to affect BBN.

Let us estimate the time scale at which we should estimate f_{H_i} . The emitted hadrons do not scatter off the ambient nucleons directly. At first the emitted high energy hadrons scatter off the background photons and electrons because they are much more abundant than the nucleons. For the most part of the epoch at the cosmic time $t \lesssim 10^4$ sec, as we can see later, it is expected that the emitted particles are quickly thermalized and they have the kinetic equilibrium distributions before they interact with the ambient nucleons. In addition as we show in Sec. IV, it is reasonable to treat the emitted hadrons to be homogeneously distributed. Then we use the thermally averaged cross sections $\langle \sigma v \rangle_{N \rightarrow N'}^{H_i}$ for the strong

²The above energy range is approximately the PBH's temperature corresponding to the lifetime $\tau_{\text{BH}} = 10^{-1} - 10^4$ sec. For $\sqrt{s} \gtrsim 350$ GeV, $t\bar{t}$ pairs would be produced and they would change the form of the charged particle multiplicity and the hadron fraction. Since we do not have the experimental data for such high energy regions, we extrapolate $\langle N_{ch} \rangle$ to the higher energy regions and we take f_{H_i} as a constant.

interaction between hadron H_i and the ambient nucleon N , where N denotes proton p or neutron n . For a hadron interaction process $N + H_i \rightarrow N' + \dots$, the strong interaction rate is estimated by

$$\begin{aligned} \Gamma_{N \rightarrow N'}^{H_i} &= n_N \langle \sigma v \rangle_{N \rightarrow N'}^{H_i} \\ &\simeq 10^8 \text{ sec}^{-1} f_N \left(\frac{\eta_i}{10^{-9}} \right) \left(\frac{\langle \sigma v \rangle_{N \rightarrow N'}^{H_i}}{10 \text{ mb}} \right) \left(\frac{T_\nu}{2 \text{ MeV}} \right)^3, \end{aligned} \quad (12)$$

where n_N is the number density of the nucleon species N , η_i is the initial baryon to photon ratio ($= n_B/n_\gamma$ at $T \gtrsim 10 \text{ MeV}$), $n_B = n_p + n_n$ denotes the baryon number density, $f_N \equiv n_N/n_B$, and T_ν is the neutrino temperature³.

Thus all we need to consider are particles with lifetime larger than $\mathcal{O}(10^{-8})$ sec. The corresponding mesons are π^+ , π^- , K^+ , K^- , and K_L and the baryons are p , \bar{p} , n , and \bar{n} . We have therefore calculated the final yield of these particles per two jets, n^{H_i} , out of Table 38.1 of [28]. The results are:

$$\begin{aligned} n^{\pi^+} &= 14.1, & n^{\pi^-} &= 14.1, \\ n^{K^+} &= 1.67, & n^{K^-} &= 1.67, & n^{K_L} &= 1.19 \\ n^p &= n^{\bar{p}} = 0.772, & n^n &= n^{\bar{n}} = 0.772. \end{aligned} \quad (13)$$

In estimating n^n we have assumed that the number of neutrons emitted directly from a jet is the same as that of protons. Then we obtain the number fraction f_{H_i} by

$$f_{H_i} = \frac{n^{H_i}}{\langle N_{ch}(\sqrt{s} = 91.2 \text{ GeV}) \rangle}. \quad (14)$$

III. HADRON INJECTION AND BBN

A. Hadron scattering off the background particles

When there are sufficient electrons and positrons in the universe ($T \gtrsim 0.025 \text{ MeV}$), it is expected that such charged mesons are quickly thermalized through the Coulomb scattering. Since the stopping time to lose the relativistic energy is estimated as

$$\tau_{ch} \simeq 10^{-14} \text{ sec} (E / \text{ GeV}) / (T / \text{ MeV})^2 \quad (15)$$

where E is the kinetic energy of a charged meson, the long-lived charged mesons are thermalized and scatter off the ambient nucleons by the threshold cross section before they decay [26]. The thermally averaged cross sections for π^\pm are obtained by [26]

³The T_ν dependence comes from that the baryon number density decrease as $n_B \propto R(t)^{-3}$ and the scale factor exactly decrease as $R(t) \propto T_\nu^{-1}$ while the universe adiabatically expands. If large entropy is produced, the above relation must be changed. In the hadron injection scenario, however, the large entropy production region is severely excluded. Therefore Eq. (12) is a good estimate of the time scale of the hadron interactions.

$$\langle\sigma v\rangle_{n\rightarrow p}^{\pi^+} = 1.7 \text{ mb}, \quad (16)$$

$$\langle\sigma v\rangle_{p\rightarrow n}^{\pi^-} = 1.5C^\pi(T) \text{ mb}, \quad (17)$$

where $C^{H_i}(T)$ is the Coulomb correction factor. Because the reaction $p^+ + \pi^- \rightarrow n + \dots$ is enhanced due to the opposite-sign charge of the initial state particles, we correct the strong interaction rates by multiplying $C^{H_i}(T)$ to that which are obtained by ignoring the Coulomb corrections. The Coulomb correction factor is estimated by

$$C^{H_i}(T) = \frac{2\pi\xi_i(T)}{1 - e^{-2\pi\xi_i(T)}}, \quad (18)$$

where $\xi_i(T) = \alpha\sqrt{\mu_i/2T}$, α is the fine structure constant and μ_i is the reduced mass of the hadron H_i and the nucleon.

The cross sections for K^- are obtained by [26]

$$\langle\sigma v\rangle_{n\rightarrow p}^{K^-} = 26 \text{ mb}, \quad (19)$$

$$\langle\sigma v\rangle_{n\rightarrow n}^{K^-} = 34 \text{ mb}, \quad (20)$$

$$\langle\sigma v\rangle_{p\rightarrow n}^{K^-} = 31C^K(T) \text{ mb}, \quad (21)$$

$$\langle\sigma v\rangle_{p\rightarrow p}^{K^-} = 14.5C^K(T) \text{ mb}. \quad (22)$$

Following Reno and Seckel [26] we ignore K^+ interaction because $n + K^+ \rightarrow p + K^0$ is the endothermic reaction which has $Q = 2.8 \text{ MeV}$.

On the other hand, among neutral kaons, K_L has a long lifetime $\mathcal{O}(10^{-8}) \text{ sec}$. Since K_L does not stop through the electro-magnetic interactions, we adopt the following strong interaction cross sections which are obtained by the initial energy distribution in the hadron fragmentation [26],

$$\langle\sigma v\rangle_{n\rightarrow p}^{K_L} = 7 \text{ mb}, \quad (23)$$

$$\langle\sigma v\rangle_{n\rightarrow n}^{K_L} = 10 \text{ mb}, \quad (24)$$

$$\langle\sigma v\rangle_{p\rightarrow n}^{K_L} = 7 \text{ mb}, \quad (25)$$

$$\langle\sigma v\rangle_{p\rightarrow p}^{K_L} = 10 \text{ mb}. \quad (26)$$

As for the emitted high energy nucleons, we should treat the thermalization process more carefully because the stopping process is not so simple. Proton and antiproton are stable and we should worry about the efficiency to lose the kinetic energy at the lower temperature. At least $T \gtrsim 0.02 \text{ MeV}$, protons are quickly thermalized through Coulomb scattering off the electrons and Inverse Compton scattering off the photons. For $t \gtrsim 3 \times 10^3 \text{ sec}$, on the other hand, the stopping process of protons proceeds through the nuclear collisions with the ambient protons and light elements. In this case such high energy protons may induce the ^4He fissions because ^4He has already been synthesized at around $t \simeq 300 \text{ sec}$. For neutron and antineutron the efficiency of the thermalization is more severe. Neutrons are efficiently stopped by the electron scattering until $T \simeq 0.09 \text{ MeV}$. Thus the late time emission of the high energy neutron would induce the light element fissions. However, in this paper we treat the neutrons as if they are approximately thermalized in the entire parameter range because we are primarily concerned with the effects of low-mass PBHs here. We follow the Reno

and Seckel's treatment that a nucleon-antinucleon pair is regarded as a meson $N\bar{N}$. Then the $N\bar{N}$ meson induces the inter-converting reactions like $N + N\bar{N} \rightarrow N' + \dots$ and the thermally averaged cross sections are given by [26]

$$\langle\sigma v\rangle_{n\rightarrow n}^{n\bar{n}} = 37 \text{ mb}, \quad (27)$$

$$\langle\sigma v\rangle_{p\rightarrow n}^{n\bar{n}} = 28 \text{ mb}, \quad (28)$$

$$\langle\sigma v\rangle_{n\rightarrow p}^{p\bar{p}} = 28 \text{ mb}, \quad (29)$$

$$\langle\sigma v\rangle_{p\rightarrow p}^{p\bar{p}} = 37 \text{ mb}. \quad (30)$$

The above treatment may underestimate the deuterium abundance because it will be produced by the hadro-dissociation of ${}^4\text{He}$ if PBHs are so massive that they continue to emit high-energy hadrons even after ${}^4\text{He}$ are formed. The hadron-induced dissociation process of the light elements will be discussed in the next paper [25]. For the other mesons and baryons whose lifetimes are much shorter, *e.g.* $\pi^0 \rightarrow 2\gamma$ with $\tau_{\pi^0} \simeq \mathcal{O}(10^{-16})$ sec, they quickly decay into the standard particles and do not influence the standard scenario.

On the other hand, for the even longer lifetime $\tau_{\text{BH}} \gtrsim 10^4$ sec, there is another interesting effects on BBN. The emitted photons or charged particles induce the electromagnetic cascade showers and produce many soft photons. Their spectrum has a cutoff at $E_\gamma^{\text{max}} \simeq m_e^2/(22T)$, where m_e is the electron mass [29]. If E_γ^{max} exceeds the binding energies of the light elements, these photons dissociate light elements and change their abundances. In fact, the energy of the photon spectrum which are produced by the PBH evaporation at $t \gtrsim 10^4(10^6)$ sec exceeds the deuterium (${}^4\text{He}$) binding energy $B_2 \simeq 2.2$ ($B_4 \simeq 20$) MeV. In this case PBH's number density and the lifetime are severely constrained by the observational data of the light element abundances [10].

B. Formulation

As we mentioned in the previous section, the hadron emission mechanism by the PBH evaporation at $t \lesssim 10^4$ sec induces extra interactions between emitted hadrons and ambient nucleons. That is, they enhance the inter-converting interaction rates between neutron and proton even after the weak interactions has already frozen out in the standard scenario and the freeze out values of n/p ratio can be increased. The time evolution of the PBH's mass is given by

$$M(t) = \begin{cases} M \left(\frac{\tau_{\text{BH}} - t}{\tau_{\text{BH}}} \right)^{\frac{1}{3}} & (\text{for } t \lesssim \tau_{\text{BH}}), \\ 0 & (\text{for } \tau_{\text{BH}} \lesssim t), \end{cases} \quad (31)$$

where M is the initial mass of PBH when it was formed.

Then the time evolution equations for the number density of a nucleon $N(= p, n)$ is represented by

$$\frac{dn_N}{dt} + 3H(t)n_N = \left[\frac{dn_N}{dt} \right]_{SBBN} - B_h J(t) (K_{N\rightarrow N'} - K_{N'\rightarrow N}), \quad (32)$$

where $H(t)$ is the cosmic expansion rate, $[dn_N/dt]_{SBBN}$ denotes the contribution from the standard weak interaction rates [16] and nuclear interaction rates, B_h is the hadronic branching ratio, $J(t)$ denotes the emission rate of the hadron jet per unit time and $K_{N\rightarrow N'}$ denotes

the average number of the transition $N \rightarrow N'$ per one hadron jet emission. The emission rate of the hadron jet is estimated by

$$J(t) = \frac{n_{\text{BH}}(t) dM(t)}{\bar{E}(t) dt}, \quad (33)$$

where $n_{\text{BH}}(t)$ is the number density of the PBHs.

Though PBHs generally emit not only quarks and gluons but also all lighter particle species than the temperature of PBH, the emitted neutrinos, photons and the other electromagnetic particles do not influence the light element abundances significantly for the relatively short lifetime. As we noted in the previous section, for $\tau_{\text{BH}} \lesssim 10^4$ sec the injection of photon or the other electro-magnetic particles do not induce the photo-dissociation of the light elements. On the other hand, the emitted neutrinos scatter off the background neutrinos and produce the electron-positron pairs. Although they also induce the electromagnetic cascade, we should not be worried about photo-dissociation for the same reason. Hence we concentrate on the effects of hadron injection in BBN epoch. Then the resultant upper bound on the abundance of PBHs, β , turns out to be proportional to B_h^{-1} . Below we analyze the case $B_h = 1$, because its magnitude is not precisely known, although we expect $B_h = \mathcal{O}(0.1 - 1)$. Anyway the constraint for other cases with $B_h \neq 1$ can easily be obtained from the above scaling law.

The average number of the transition $N \rightarrow N'$ per jet is expressed by

$$K_{N \rightarrow N'} = \sum_{H_i} N^{H_i} R_{N \rightarrow N'}^{H_i}, \quad (34)$$

where H_i runs the hadron species which are relevant to the nucleon inter-converting reactions, N^{H_i} denotes the average number of the emitted hadron species H_i per jet which is given by Eq. (10) and $R_{N \rightarrow N'}^{H_i}$ denotes the probability that a hadron species H_i induces the nucleon transition $N \rightarrow N'$. The transition probability is estimated by

$$R_{N \rightarrow N'}^{H_i} = \frac{\Gamma_{N \rightarrow N'}^{H_i}}{\Gamma_{dec}^{H_i} + \Gamma_{abs}^{H_i}}, \quad (35)$$

where $\Gamma_{dec}^{H_i} = \tau_{H_i}^{-1}$ is the decay rate of the hadron H_i , $\Gamma_{abs}^{H_i}$ is the total absorption rate of H_i . For K_L , which is not stopped, the decay rate is approximately estimated by $\Gamma_{dec}^{K_L} = m_{K_L}/E_{K_L} \tau_{K_L}^{-1}$ where E_{K_L} is the averaged energy of the emitted K_L .

C. Observational constraints

As we mentioned in the previous subsection, the hadron injection increases the freeze-out value of n/p ratio. The remaining neutrons are included in the deuteriums rapidly and it burns into ^4He . Since the effects of the late time hadron emission tend to increase D and ^4He we can constrain mass and abundance of PBHs comparing the yield with the observational light element abundances. In this subsection we briefly review the observational data of the light elements D, ^4He and ^7Li .

The primordial deuterium is measured in the high redshift QSO absorption systems. Because it is expected that such a Lyman limit system is not contaminated by any galactic

or stellar chemical evolution, we regard it as a primordial component. At present we have two class of the observational D values, Low D and High D. However, since it is premature to determine which component is primordial, we consider both of two cases in this paper. Burles and Tytler observed clouds at $z = 3.572$ towards Q1937-1009 and at $z = 2.504$ towards Q1009+2956 and they obtained [30]

$$D/H = (3.39 \pm 0.25) \times 10^{-5} : \text{Low D}, \quad (36)$$

where D/H denotes the deuterium number fraction and the error is the 1σ value. On the other hand, Webb et al. reported the higher abundance in relatively low redshift absorption systems at $z = 0.701$ towards Q1718+4807, $D/H \simeq \mathcal{O}(10^{-4})$ [31]. Tytler et al. also observed the same clouds and obtain the high deuterium abundance independently [32],

$$D/H = (0.8 - 5.7) \times 10^{-4} : \text{High D}, \quad (37)$$

where the uncertainty is 2σ .

The primordial component of the ^4He mass fraction Y_p is measured in the low metallicity extragalactic HII region. In addition to the primordial component, ^4He is also produced in stars together with Oxygen and Nitrogen through the stellar evolution mechanism. Therefore in order to obtain the primordial component from the observational data we should regress to the zero metallicity for the observed ^4He values. Olive, Skillman and Steigman [33] adopted 62 blue compact galaxies (BCG) observations and they obtained the relatively ‘‘Low’’ abundance, $Y_p \simeq 0.234$. However, Thuan and Izotov [34] pointed out that the effect of the HeI stellar absorption, which was not considered properly in [33], is very important and they reported the relatively ‘‘High’’ value, $Y_p = 0.245 \pm 0.004$. Recently Fields and Olive [35] reanalyzed the observational data and they reported

$$Y_p = 0.238 \pm (0.002)_{stat} \pm (0.005)_{syst}, \quad (38)$$

where the errors are the 1σ values.

The primordial value of $^7\text{Li}/\text{H}$ is measured in the Pop II old halo stars. Since the low mass stars, *i.e.* the low temperature stars, have the deep convective zone, the primordial component should be considerably depleted in the warm interiors. For the large mass stars which have the relatively high effective surface temperature $T_{eff} \gtrsim 5500\text{K}$, it is known that the primordial components are not changed and they have a ‘‘plateau’’ of the $^7\text{Li}/\text{H}$ as a function of T_{eff} . On the other hand it is also reported that $^7\text{Li}/\text{H}$ abundances decrease along with Iron fraction $[\text{Fe}/\text{H}]$. For the plateau stars, however, the ^7Li abundances are not changed with decreasing $[\text{Fe}/\text{H}]$ for $[\text{Fe}/\text{H}] \lesssim -1.5$. Bonifacio and Molaro observed 41 plateau stars and reported [36]

$$\log_{10}(^7\text{Li}/\text{H}) = -9.76 \pm (0.012)_{stat} \pm (0.05)_{syst} \pm (0.3)_{add}, \quad (39)$$

where $^7\text{Li}/\text{H}$ denotes ^7Li number fraction, the errors are 1σ values and we take an additional systematic error $\Delta \log_{10}(^7\text{Li}/\text{H})_{add} = 0.3$, for fear that we may underestimate the stellar depletion and the production by the cosmic ray spallation.

In order to get the conservative bound for the hadron injection induced by PBH evaporation, we adopt the following mild observational bounds here,

$$Y_p \leq 0.252 (2\sigma), \quad (40)$$

$$D/H \leq 4.0 \times 10^{-5} (2\sigma) \quad \text{for LowD} \quad (41)$$

$$D/H \leq 5.7 \times 10^{-4} (2\sigma) \quad \text{for HighD}, \quad (42)$$

$$3.3 \times 10^{-11} \leq {}^7\text{Li}/H \leq 9.2 \times 10^{-10} (2\sigma), \quad (43)$$

where we summed all the errors in quadrature.

IV. RESULTS

In this section we compare the theoretical predictions of the light-element abundances in the hadron injection scenario with the observational constraints. Now we have three free parameters, the baryon to photon ratio η , the PBH's lifetime τ_{BH} , and the initial number density of the PBH normalized by the entropy density, s , $Y_{\text{BH}} \equiv n_{\text{BH}}/s$. We start the BBN calculation at the cosmic temperature $T = 100$ MeV. Since η is the value at present time, the initial value η_i should be set to an appropriate value which turns out to the present η after the possible entropy production due to PBH evaporation and the photon heating due to e^+e^- annihilation. As we noted in the previous sections, the lifetime τ_{BH} characterizes not only the decay epoch, but also the PBH's initial mass M and the initial PBH temperature T_{BH} . Here we can relate Y_{BH} to the initial mass fraction β by the following equation:

$$\beta = 5.4 \times 10^{21} \left(\frac{\tau_{\text{BH}}}{1 \text{ sec}} \right)^{\frac{1}{2}} Y_{\text{BH}}. \quad (44)$$

Since the hadron injection tends to increase the produced D and ${}^4\text{He}$ abundances in the present situation, the parameter range of η is necessarily restricted to a narrow region if we adopt a set of the observational upper bounds for D and ${}^4\text{He}$. First we discuss the case of ‘‘LowD’’ and take Eqs. (40), (41) and (43) as a first set of the observational constraints. In this case the baryon-to-photon ratio is restricted in $\eta = (4.7 - 8.6) \times 10^{-10}$.

In Fig. 2 we plot the upper bounds for β which come from the observational constraints of ${}^4\text{He}$, D and ${}^7\text{Li}$ for the PBH mass $M = 10^8 - 3 \times 10^{10} \text{g}$ at $\eta = 6.0 \times 10^{-10}$. The above mass range corresponds to the lifetime $\tau_{\text{BH}} = 4.4 \times 10^{-4} - 10^4 \text{sec}$. As we noted earlier, the shorter lifetime, $\tau_{\text{BH}} \lesssim 10^{-2} \text{sec}$, do not affect the freeze-out value of n/p and do not change any predictions of SBBN. However, if the lifetime becomes $\tau_{\text{BH}} \gtrsim 10^{-2} \text{sec}$, the freeze-out value of n/p ratio is increased by the hadron-induced inter-converting interactions and the produced neutron increases the ${}^4\text{He}$ abundance because most of the free neutrons burned into ${}^4\text{He}$ through D. Then PBH abundance is strongly constrained by the upper bound of the observational ${}^4\text{He}$ abundance. For $\tau_{\text{BH}} \gtrsim 10^2 \text{sec}$, since the produced free D can no longer burn into ${}^4\text{He}$, the extra free neutrons remain in D. Then β is severely constrained by the upper bound of the observational D/H. Though ${}^7\text{Li}$ abundance traces D abundance for the longer lifetime $\tau_{\text{BH}} \gtrsim 10^2 \text{sec}$ and is produced more than SBBN at the relatively high η ($\gtrsim 3 \times 10^{-10}$), the constraint is much weaker than D.

In Fig. 3 we plot the most conservative bounds in the parameter region $\eta = (4.7 - 8.6) \times 10^{-10}$. For $\tau_{\text{BH}} \lesssim 4 \times 10^2 \text{sec}$ such a bound is obtained by Y_p at $\eta = 4.7 \times 10^{-10}$. For $4 \times 10^2 \lesssim \tau_{\text{BH}} \lesssim 10^4 \text{sec}$, the prediction of D/H at $\eta = 8.6 \times 10^{-10}$ gives the most conservative bound for β , but constraints in this region is not quantitatively accurate because we did not include spallation of ${}^4\text{He}$ produced.

Second we discuss the other case “HighD” and adopt a second set of the observational constraints Eqs. (40), (42), and (43). The upper bounds for D and ${}^4\text{He}$ restrict the baryon to photon ratio necessarily within $\eta = (0.90 - 8.6) \times 10^{-10}$. In Fig.4, we plot the upper bounds for β as a function of PBH mass at $\eta = 2.0 \times 10^{-10}$. Because the observational upper bound for D is very weak, the allowed region for $\tau_{\text{BH}} \gtrsim 10^2$ sec are enlarged. Since the predicted ${}^4\text{He}$ abundance has the log dependence for η , the constraint which comes from Y_p is not changed very much compared with the case of $\eta = 6.0 \times 10^{-10}$. In Fig. 5 we plot the most conservative upper bounds for β in the parameter space $\eta = (0.90 - 8.6) \times 10^{-10}$. As we mentioned above, the D constraint is not strict because of the weak observational upper bound. On the other hand, the constraint from ${}^7\text{Li}/\text{H}$ is the most severe for $\tau_{\text{BH}} \gtrsim 10^2$ sec because ${}^7\text{Li}/\text{H}$ are almost not allowed to be produced at $\eta = 0.90 \times 10^{-10}$.

Finally we estimate the number of PBHs within the neutron diffusion length $d_n(t)$ at $t = \tau_{\text{BH}}$. The neutron diffusion length is given by [37]

$$d_n(t) = 5.8 \times 10^2 \left(\frac{T}{1 \text{ MeV}} \right)^{-\frac{5}{2}} \left(\frac{\sigma_t}{3 \times 10^{-30} \text{ cm}} \right)^{-\frac{1}{2}}, \quad (45)$$

where σ_t is a transport cross section. Using Eq. (8), the number of PBHs within the horizon length at $t = \tau_{\text{BH}}$ is given by

$$N_H(\tau_{\text{BH}}) = \left(\frac{\tau_{\text{BH}}}{t_{\text{form}}} \right)^{\frac{3}{2}} \beta = 7.7 \times 10^{46} M_{10}^3 \beta. \quad (46)$$

Then the number of PBHs within the neutron diffusion length is estimated by

$$N_d(\tau_{\text{BH}}) = \begin{cases} 1.2 \times 10^{21} \beta, & (\text{for } \tau_{\text{BH}} = 1 \text{ sec}), \\ 2.3 \times 10^{46} \beta, & (\text{for } \tau_{\text{BH}} = 10^3 \text{ sec}). \end{cases} \quad (47)$$

Compared with Figs. 2 – 5, we can see that there exist sufficiently many PBHs within the neutron diffusion length in the relevant parameter spaces in which we are interested and the number of PBHs is observationally constrained. Therefore it is justified that we can take the emitted hadrons as a homogeneously distributed background.

V. CONCLUSION

We have investigated the influence of hadron injection from evaporating PBHs in the early stage of the BBN epoch ($t \simeq 10^{-3} - 10^4$ sec). The above lifetimes correspond to the mass range of PBHs $M \simeq 10^8 - 3 \times 10^{10}$ g. When quark-antiquark pairs or gluons are emitted from PBH, they immediately fragment into a lot of hadrons (pions, kaons and little nucleons) and the produced hadron jets are injected into the thermal plasma which is constituted by photons, electrons and nucleons. After the emitted hadrons are sufficiently stopped through the electro-magnetic interaction with the ambient photons and electrons, they can scatter off the ambient nucleons and they inter-convert proton and neutron each other. As a result more neutrons are produced and the synthesized light element abundances are drastically changed. In particular, ${}^4\text{He}$ and D abundances are very sensitive to the neutron abundance and tend to increase in this scenario. Comparing with the observational data, we can

constrain PBH's density and their lifetime. The hadron injection which are originated by the direct quark-antiquark pairs or gluons emission from PBHs has never considered at all in the literature. In this paper we pointed out that the hadron induced inter-converting interactions between protons and neutrons are very important and the energy density of PBH is severely constrained by the observational data.

We obtain the following upper bounds for the initial mass fraction of PBH β as a function of the initial mass of PBH when they are formed

$$\beta \lesssim 10^{-20} \quad (\text{for } 10^8 \text{g} \lesssim M \lesssim 10^{10} \text{g}) \quad (48)$$

$$\beta \lesssim 10^{-22} \quad (\text{for } 10^{10} \text{g} \lesssim M \lesssim 3 \times 10^{10} \text{g}). \quad (49)$$

Here we adopt the case of “lowD” because the produced D is more severely constrained, and we take the most conservative bounds which are independent of the baryon to photon ratio.

ACKNOWLEDGMENTS

We wish to thank O. Biebel for providing the experimental data of the charged particle multiplicity and his detailed explanations of them. We are also grateful to M. Kawasaki, M.M. Nojiri, S. Orito, and N. Sasao for useful communications. This work was partially supported by the Monbusho Grant-in-Aid for Scientific Research Nos. 10-04502 (KK) and 11740146 (JY).

REFERENCES

- [1] Ya.B. Zel'dovich and I.D. Novikov, *Soviet Astronomy* **10**, 602 (1967); S.W. Hawking, *Mon. Not. R. astr. Soc.* **152**, 75 (1971); B.J. Carr, *Astrophys. J.* **201**, 1 (1975).
- [2] C. Alcock et al., *Nature*, **365**, 623 (1990); *Phys. Rev. Lett.* **74**, 2867 (1995); *Astrophys. J.* **486**, 697 (1997); E. Aubourg et al., *Nature*, **365**, 623 (1993); *Astron. Astrophys.* **301**, 1 (1995).
- [3] J. Yokoyama, *Astron. Astrophys.* **318**, 673 (1997); *Phys. Rev. D* **58**, 083510 (1998); *Phys. Rep.* **307**, 133 (1998).
- [4] S.W. Hawking, *Nature* **248**, 30 (1974); *Comm. Math. Phys.* **43**, 199 (1975).
- [5] B.J. Carr, *Astrophys. J.* **206**, 8 (1976).
- [6] B.V. Vainer and P.D. Nasel'skii, *Astron. Zh.* **55**, 231 (1978) [*Sov. Astron.* **22**, 138 (1978).]
- [7] S. Miyama and K. Sato, *Prog. Theor. Phys.* **55**, 1012 (1978).
- [8] Ya.B. Zel'dovich, A.A. Starobinskii, M.Yu. Khlopov, and V.M. Chechëtkin, *Pis'ma Astron. Zh.* **3**, 208 (1977) [*Sov. Astron. Lett.* **3**, 110 (1977).]
- [9] B.V. Vainer, O.V. Dryzhakova, and P.D. Nasel'skii, *Pis'ma Astron. Zh.* **4**, (1978) [*Sov. Astron. Lett.* **4**, 185 (1978).]
- [10] D. Lindley, *Mon. Not. Roy. Astron. Soc.* **193**, 593 (1980).
- [11] Ya.B. Zel'dovich, A.A. Starobinskii, *JETP Lett.* **24**, 571 (1976).
- [12] J.H. MacGibbon, *Nature* **329**, 308 (1987); J.H. MacGibbon and B.J. Carr, *Astrophys. J.* **371**, 447 (1991).
- [13] M.B. Bowick, S.B. Giddings, and J.A. Harvey, *Phys. Rev. Lett.* **61**, 2823 (1988); J.D. Barrow, E.J. Copeland, and A.R. Liddle, *Phys. Rev.* **D46**, 645 (1992).
- [14] J.D. Barrow and B.J. Carr, *Phys. Rev. D* **54**, 3920(1996).
- [15] A.M. Green and A.R. Liddle, *Phys. Rev. D* **56**, 6166(1997).
- [16] For a review of BBN, see, *e.g.* T.P. Walker, G. Steigman, D.N. Schramm, K.A. Olive, and H.-S. Kang, *Astrophys. J.* **376** (1991) 51; K.A. Olive, G. Steigman, and T.P. Walker, astro-ph/9905320
- [17] J.H. MacGibbon and B.J. Carr, *Astrophys. J.* **371**, 447(1991) ; B.J. Carr and J.H. MacGibbon, *Phys. Rept.* **307**, 141(1998).
- [18] J.C. Niemeyer and K. Jedamzik, *Phys. Rev. Lett.* **80**, 5481 (1998); *Phys. Rev.* **D59**, 124013 (1999).
- [19] M. Shibata and M. Sasaki, gr-qc/9905064, To be published in *Phys. Rev. D*.
- [20] J. Yokoyama, *Phys. Rev.* **D58**, 107502 (1998); A.M. Green and A.R. Liddle, astro-ph/9901268; H.I. Kim, astro-ph/9907372.
- [21] D.N. Page, *Phys. Rev. D* **13**, 198(1976); **14**, 3260(1976); **16**, 2402(1977).
- [22] J.H. MacGibbon and B.R. Webber, *Phys. Rev. D* **41**, 3052(1990).
- [23] J.H. MacGibbon, *Phys. Rev. D* **44**, 376(1991).
- [24] S. Dimopoulos, R. Esmailzadeh, L. Hall, and G. Starkman, *Phys. Rev. Lett.* **60**, 7 (1988); *Astrophys. J.* **330**, 545 (1988); *Nucl. Phys.* **B311**, 699 (1988/89).
- [25] K. Kohri and J. Yokoyama, in preparation.
- [26] M. H. Reno and D. Seckel, *Phys. Rev.* **D37**, 3441 (1988)
- [27] W. Furmanski, R. Petronzio and S. Pokorski, *Nucl. Phys.* **B155**, 253 (1979); A. Bassetto, M. Ciafaloni and G. Marchesini, *Phys. Lett.* **B83**, 207 (1979);

- K. Konishi, Rutherford Lab. Rep RL 79-035 (1979);
A. H. Mueller, Phys. Lett. **B104**, 161 (1981); Nucl. Phys. **B213**, 85 (1983).
- [28] C. Caso *et al.*, Particle Data Group, *Euro. Phys. J. C* **3**, 1 (1998).
- [29] E. Holtmann, M. Kawasaki, K. Kohri, and T. Moroi, Phys. Rev. **D60**, 023506 (1999).
- [30] S. Burles and D. Tytler, *Astrophys. J.* **507**, 732 (1998).
- [31] J. K. Webb *et al.*, *Nature* **388**, 250 (1997).
- [32] D. Tytler, S. Burles, L. Lu, X-M. Fan and A. Wolfe, *Astron. J.* **117**, 63 (1999).
- [33] K.A. Olive, E.D. Skillman, and G. Steigman, *Astrophys. J.* **483**, 788 (1997).
- [34] Y.I. Izotov, T.X. Thuan, and V.A. Lipovetsky, *Astrophys. J. Suppl. Series*, **108**, 1 (1997); Y.I. Izotov and T.X. Thuan *Astrophys. J.*, **500**, 188 (1998).
- [35] B.D. Fields and K.A. Olive, *Astrophys. J.*, **506**, 177 (1998).
- [36] P. Bonifacio and P. Molaro, *Mon. Not. Roy. Astron. Soc.* **285**, 847 (1997).
- [37] J.H. Applegate and C.J. Hogan, Phys. Rev. **D31**, 3037 (1985).

FIGURES

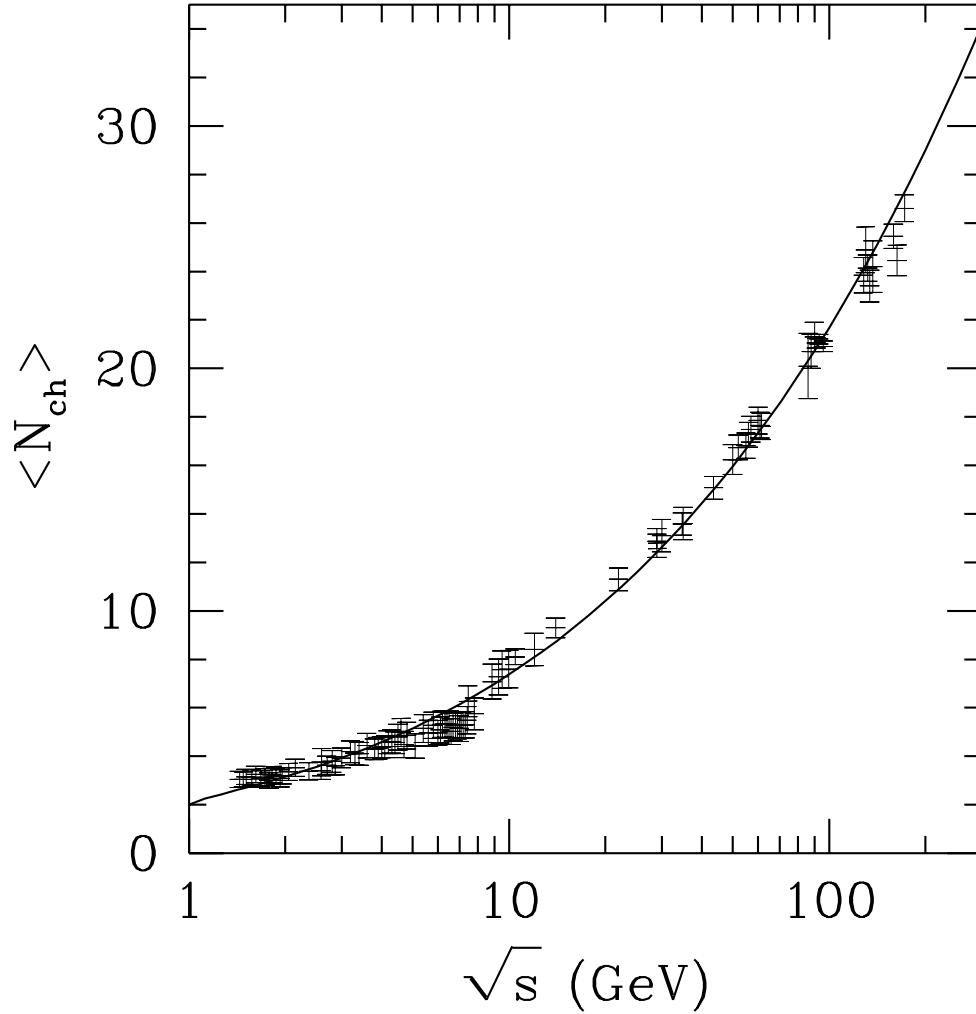


FIG. 1. Plot of the charged particle multiplicity $\langle N_{ch} \rangle$ for the center of mass energy \sqrt{s} . At about $\sqrt{s} \simeq 91.2$ GeV the experimental data are spread horizontally by authors. We assigned systematic errors of 10% for $\sqrt{s} = 1.4 - 7.8$ GeV .

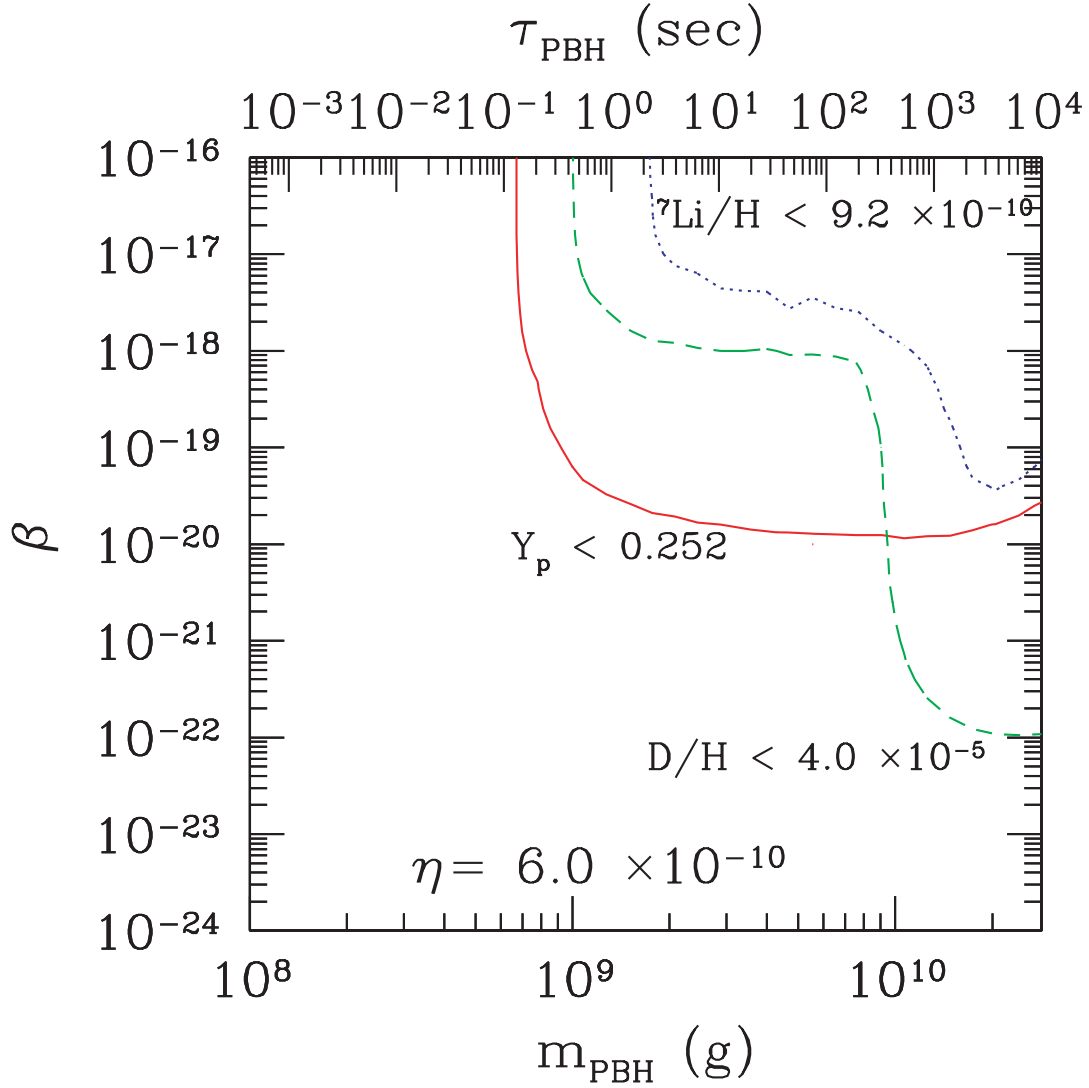


FIG. 2. Upper bounds for β which come from the observational constraints of ^4He (solid line), D (dashed line) and ^7Li (dotted line) as a function of the PBH's mass at $\eta = 6.0 \times 10^{-10}$. Here we take “LowD” as a deuterium observational constraints.

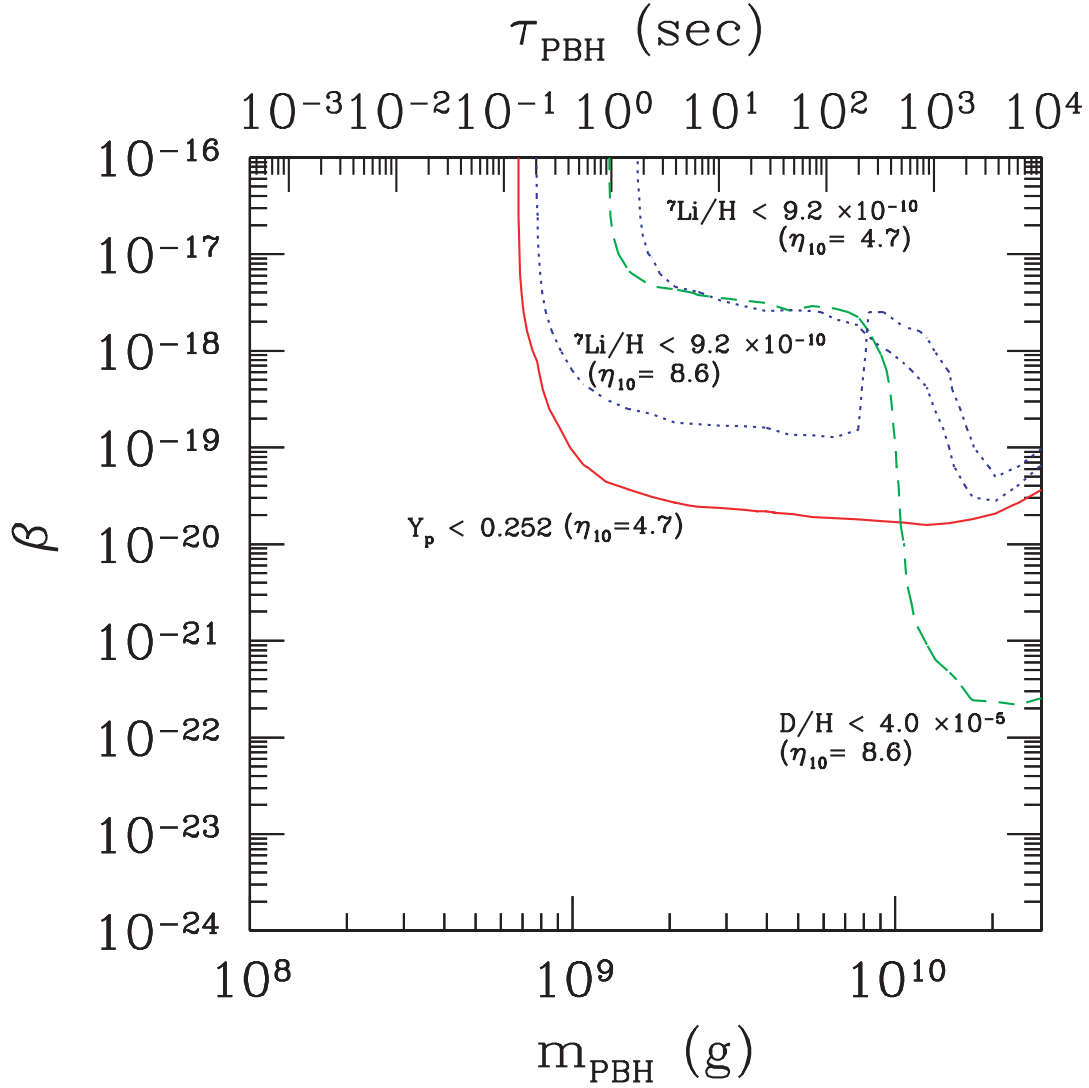


FIG. 3. The most conservative upper bounds for ${}^4\text{He}$ (solid line), D (dashed line) and ${}^7\text{Li}$ (dotted line) as mild as possible in the parameter region $\eta_{10} = 4.7 - 8.6$, where $\eta_{10} \equiv \eta \times 10^{10}$. Here we take “LowD” as a deuterium observational constraint.

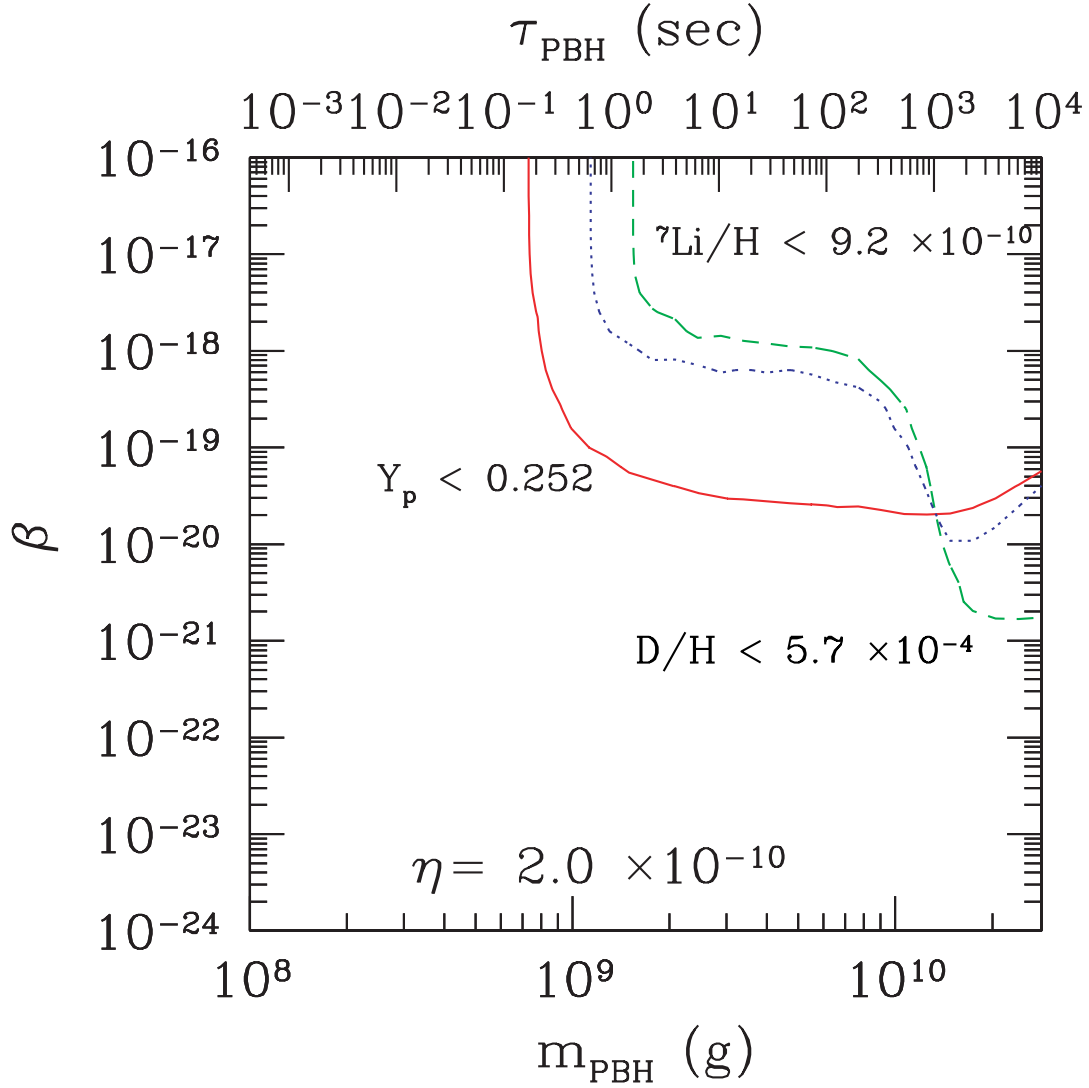


FIG. 4. Upper bounds for β which come from the observational constraints of ${}^4\text{He}$ (solid line), D (dashed line) and ${}^7\text{Li}$ (dotted line) as a function of the PBH's mass at $\eta = 2.0 \times 10^{-10}$. Here we take “HighD” as a deuterium observational constraints.

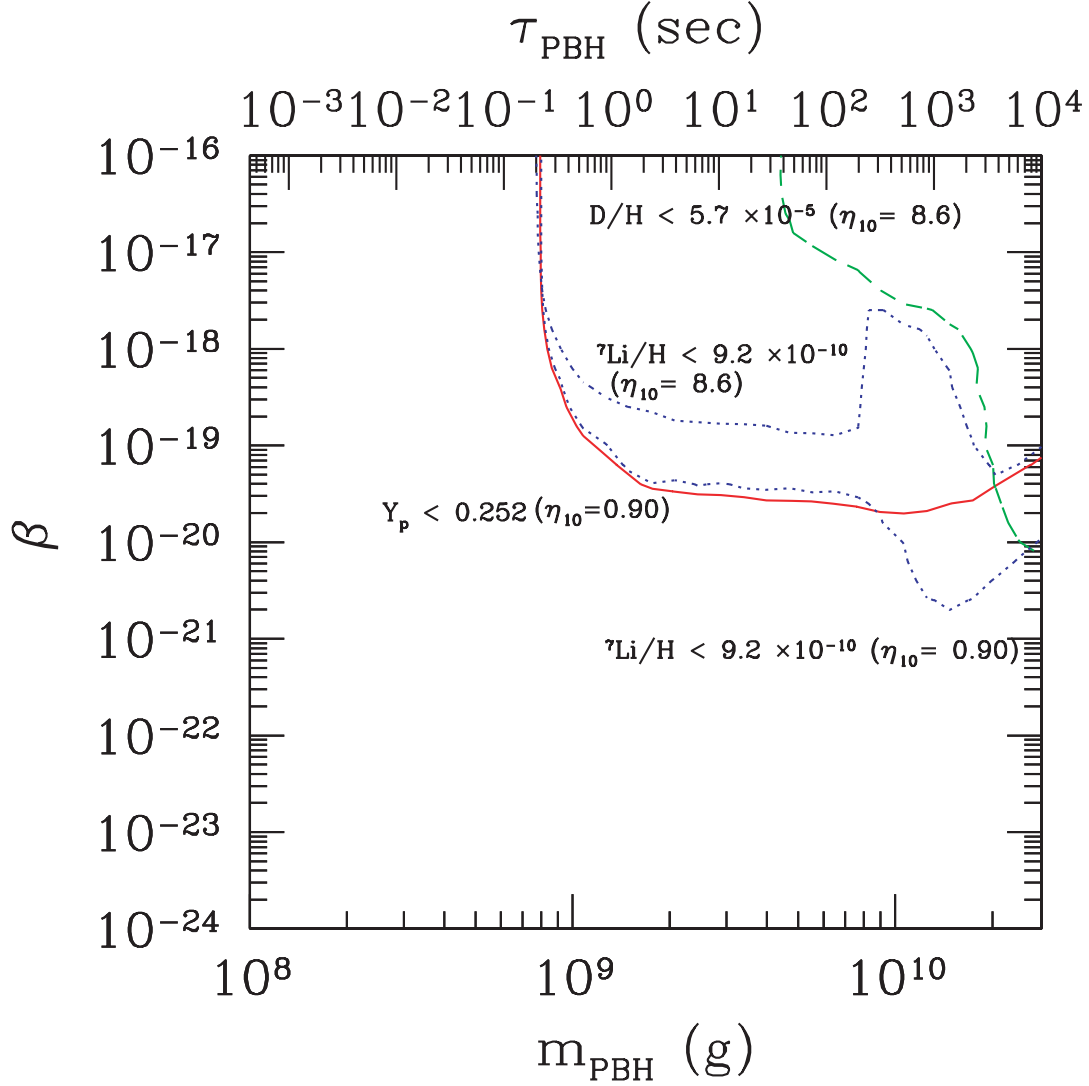


FIG. 5. The most conservative bounds for ${}^4\text{He}$ (solid line), D (dashed line) and ${}^7\text{Li}$ (dotted line) as mild as possible in the parameter region $\eta_{10} = 0.90 - 8.6$, where $\eta_{10} \equiv \eta \times 10^{10}$. Here we take “HighD” as a deuterium observational constraints. .